Journal Pre-proof

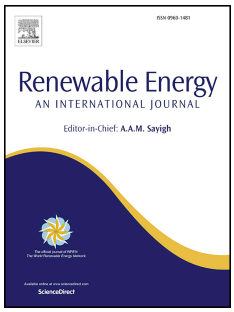

Effect of the absorber surface roughness on the performance of a solar air collector: An experimental investigation

Biplab Das, Jayanta Deb Mondol, Suman Debnath, Adrian Pugsley, Mervyn Smyth, A. Zacharopoulos

PII: S0960-1481(20)30061-6

DOI: https://doi.org/10.1016/j.renene.2020.01.056

Reference: RENE 12918

To appear in: *Renewable Energy*

Received Date: 6 August 2019

Revised Date: 24 December 2019

Accepted Date: 12 January 2020

Please cite this article as: Das B, Mondol JD, Debnath S, Pugsley A, Smyth M, Zacharopoulos A, Effect of the absorber surface roughness on the performance of a solar air collector: An experimental investigation, *Renewable Energy* (2020), doi: https://doi.org/10.1016/j.renene.2020.01.056.

Authors'Contribution

- The 1st author and also the corresponding author is responsible for ensuring that the descriptions are accurate and agreed by all authors.
- 2nd author helped in the development of methodology.
- 3rd author contributed for the extensive literature review.
- 4th author contributed to develop the methodology and critical analysis of the results.
- 5th author contributed to the experimentation and selection of proper governing parameters.
- 6th author contributed to the critical analysis of the results.

Effect of the absorber surface roughness on the performance of a solar air collector: an experimental investigation

[1,2*] Biplab Das; [1]Jayanta Deb Mondol; [2]Suman Debnath; [1]Adrian Pugsley; [1]Mervyn Smyth; [1]A Zacharopoulos

[1]Belfast School of Architecture and the Built Environment, Centre for Sustainable Technology, Ulster University, Northern Ireland, UK.

[2]Department of Mechanical Engineering, National Institute of Technology Silchar, Assam-788010, India

**corresponding author:*

Email: biplab.2kmech@gmail.com/ b.das@ulster.ac.uk Ph (m) - +44 7563225168

Acknowledgement: Fund received from the DBT, Govt of India, under Overseas Associateship is highly acknowledged. Authors also would like to acknowledge the Ulster University for providing access to the CST laboratory facilities for carrying out the tests. One of the authors (Biplab Das) would like to thank NIT Silchar for sanctioning the leave to avail of the fellowship.

Effect of the absorber surface roughness on the performance of a solar air collector: an experimental investigation

Abstract:

Solar air collectors (SAC) convert the available solar energy into useful thermal energy for different heating applications such as drying, space heating, hot water etc. The study aims to enhance the thermal performance of a flat plate SAC by modifying the absorber surface. The experimental performance of two variant SACs (a sand coated absorber to increase surface roughness and a conventional plain absorber) was compared under controlled laboratory conditions The experimental tests were performed under a solar simulator for radiation levels of 400, 600, and 800 W/m^2 and variable air mass flow rate ranging from 0.01 to 0.02 kg/s/m^2. Results indicated that increasing the air flow rate by 90% enhanced the thermal efficiency on a plain absorber SAC by almost 68%, and the rate of increase was higher for the sand coated absorber. SAC with the sand coated absorber provided additional surface area resulting in an increase in the effective heat transfer. The thermal efficiency of the collector was improved by up to 17% for the sand coated absorber compared to the plain absorber. The absolute thermal efficiency of the SAC varied from 19% to 41% under the different tests conditions.

Keyword: *Solar air collector; sand coated absorber; thermal efficiency; effective thermal efficiency; correlation*

1. Introduction

Solar air collectors (SACs) convert the available solar energy into useful thermal energy commonly for drying and space heating. SACs can be classified based on the characteristics of the collector cover plate, absorber plate materials use surface configuration, integrated or hybrid, number of flow-passes, flow pattern and application. The purpose of the design variation is to increase the heat transfer inside the SAC.

Hegazy [1] investigated SACs to evaluate it performance using variable width and fixed length collectors. Results indicated that a trapezoidal absorber plate is far better than a concave absorber. Hernández and Quiñonez [2] presented double pass parallel and counter flow SACs through an analytical study. It was observed that the performance of SACs for counter and parallel flow remained the same at higher flow rates. The performance of a perforated glazed solar collector with mass flow rates between 0.017 and 0.036 kg/s was evaluated by Vaziri et al. [3]. The maximum and minimum collector efficiency for SAC with black and white coloured absorber was found to be 85% and 54%, respectively. Aissaoui et al. [4] studied the performance of a flat

plate SAC both experimentally and computationally. The thermal efficiency was found to vary between 22% and 40%. Soriga and Badescu [5] highlighted that the thermal inertia of a solar air heater ranged between 0.4 to 0.7. Sun et al. [6] presented a mathematical model for SACs by varying the mass flow rate from 0.02 to 0.05 kg/s and solar radiation between 100 and 1000W/m^2. Thermo-hydraulic efficiency was found to vary between 35% and 55%. Abdullah et al. [7] determined that the thermal efficiency of a semi-circular plastic SAC was 80% which was higher than a flat (35%) and triangular (25%) cover. Caliskan [8] performed a techno-economic investigation of a SAC and found the energy efficiency and exergy efficiency of 25.4% and 0.73%, respectively. Kabeel et al. [9] reported that for a double pass flow SAC with nickel-tin selective coated absorber provide 29.23% higher efficiency than only black paint. Debnath et al. [10] reported that the efficiency of a flat plate SAC was 37.55% at a mass flow rate of 0.014 kg/s for solar radiation between 300 and 900 W/m^2 under North-East (NE) Indian climatic conditions..

The performance enhancement of SACs through surface modification has been studied by many researchers. The main aim is to break the formation of boundary layer, to increase the rate of redistribution of the flow and to reduce losses. A detailed review of earlier studies was presented by Lanjewar et al. [11] and Alam and Kim [12].

Prasad and Saini [13] investigated the effect of artificial roughness on the pressure drop and heat transfer of a SAC. Results indicated that heat transfer was enhanced by up to 2.4 times whilst the friction factor increased by 4.25 times. El-Sebaii et al. [14] investigated double pass SACs with flat and V-corrugated absorber plates. The V-corrugated collector provided 11-14% better efficiency than the flat plate SAC. Ho et al. [15] investigated theoretically an upward type SAC having a finned absorber with externally recycled air. It was found that the externally recycled air strengthened the heat convection and improved the thermal performance. Ho et al. [16] also compared a double pass SAC with fins and baffles and reported that the baffles had a greater impact when compared to the fins. Benli [17] concluded that a corrugated absorber provided an efficiency of 55% at a flow rate of 0.05 kg/s from five different shapes of absorber surface (flat, corrugate, reverse corrugate, trapeze and reverse trapeze).

Ravi and Saini [18] performed an experimental investigation on double pass SAC with flat and V-corrugated absorber to obtain Nu and friction factor. Results showed a 4.5 times increment in Nu number for the V-corrugated absorbers compared to the flat plate, whilst the friction factor increased by 3.1. An experimental investigation conducted by Kabeel et al. [19] on SACs using flat and V-corrugated absorber with PCM based energy storage showed that a collector with V-corrugated absorber with PCM storage was 12% to 21% more efficient than a flat plate SAC with

and without PCM. Effectively Ho et al. [20] reported that for a V-corrugated SAC with double pass recycling, the collector performance improved at higher recycle ratios and mass flow rates compared to a conventional SAC. Kabeel et al. [21] investigated SAC with flat plate, finned, baffled, and baffled fin absorber and found that the maximum efficiency of a baffled fin absorber was 83.8% at flow rate of 0.04 kg/s. A comparative study conducted by Sevik and Abuska [22] on SACs having flexible aluminium foil absorber with and without glass covers showed that a maximum efficiency of 81.3% was obtained for an aluminium foil absorber at a flow rate of 0.044 kg/s. Debnath et al. [23] compared the performance of SACs with plain and wavy absorbers in NE India with variable flow rates, tilt angles, and number of glazing layers, the efficiency of the wavy absorber was 14% higher than the flat plate SAC.

Boukadoum and Benzaoui [24] carried out a CFD study to determine the enhancement of the heat transfer rate using rectangular transverse type ribs inside the collector. Results indicated that the rate of heat transfer is increased without huge losses in friction. A correlation between the Nusselt numbers and friction factor for a triangular SAC having rectangular chamfered ribs were proposed by Kumar et al. [25] based on the CFD study by Sharma and Kalamkar [26] conducted an experimental study on SAC having four different thin rib configurations under forced convection to estimate the thermo-hydraulic performance, friction factor, and heat transfer. A computational analysis of a flat-plate SAC operating with a recycled working fluid (0-7 times) showed that the efficiency was increased by 118% due to recycling of the working fluid by 7 times [27-28]. Naphon [29] performed an analytical study to determine the effect of fin height, number of fins, and air flow rate on the performance of a SAC.

Mohamad [30] observed that by minimizing the collector losses especially losses through the glass cover, the collector thermal efficiency was around 75%. Ozgen et al. [31] found that the collector efficiency increased by up to 45% at peak solar conditions by attaching aluminium cans with a flat absorber. Omojaro and Aldabbagh [32] studied the performance of single and double pass SACs with finned and wire mesh absorbers. Double pass collector provided up to 19% higher efficiency than that of plain absorber. A maximum efficiency of a conical spring attached to a flat plate SAC was around 68% as reported by Abuska and Akgul [33] and Abuşka [34]. Ansari and Bazargan [35] reported that a ribbed SAC provided up to 9% higher overall thermal efficiency compared to a flat plate SAC. Velmurugan and Kalaivanan [36] studied a single pass SAC with different geometrical configurations. The maximum efficiency was found to be 76.46%. Ahmadi et al. [37] reported that the thermal performance of a collector enhanced by

18.87% by using graphene nanoplatelets. Table 1 summarises the thermal efficiency of different configurations of SAC.

Previous studies indicate that the design enhancements such as the incorporation of fins, baffles, vortex generator, nanopatlets, etc. on the absorber enhances the performance of the SAC. However, these methods are expensive and complex thus has limited commercial applications. To the best of knowledge of the authors the only work available on solar collector with sand coated absorber has been reported by Lati et al. [38], in which air flow under the absorber plate at a fixed mass flow rate. This study aims to improve the thermal performance of a SAC by augmenting the absorber surface with a sand coating over the absorber surface, offering a more cost-effective enhancement.

2. Experimental Set Up

The experimental setup of the SAC including temperature sensors position is shown in Fig. 1. The cross-sectional area of the collector was 1.44 m^2 with a space for absorber plate of 0.97 m ×0.97 m. Other than the absorber plate, the technical specifications of both the SACs were the same. The sides and back of the collector were insulated with thermocol of 0.02 m thick, and the whole system was made up of plywood with the thickness of 0.015 m. Both absorber plates were coated with black paint to increase the absorptivity. For the sand coated absorber, first the black paint and preheated sand of 35-371 micron were mixed by agitating until the sand got a homogeneous mixture and then coated sand were painted over the aluminium absorber and let to dry up. The size and spatial distribution of the used sand is shown in Fig. 2. To reduce the top losses and to drive the air over the absorber, a glazing cover made of acrylic perspex sheet of 0.005 m thick was used. At the inlet section of SAC two DC fans powered from a DC source were used to force air over the absorber. The speed of the fan was controlled by varying the input power supply.

Tests were performed under a solar simulator at the CST laboratory at Ulster University. In the present study the radiation level was varied form 400 W/m^2 to 800 W/m^2. A pyranometer was used to measure the radiation level at nine different points on the collector surface to check the uniformity of radiation on the surface before each set of tests. Radiation level was observed to vary by 10%. The average intensity on the collector surface varied between ±15 W/m^2. The inclination of the SAC and the solar simulator lamp array were kept fixed at 45º. A digital anemometer was used to measure the exit air velocity. Temperature readings from the T-type thermocouples were recorded by a data logger (data taker, DT85) at 30 sec intervals. The

accuracy of the instruments and corresponding uncertainties are calculated using the following equation and for each of the parameters are presented in Tables 2 & 3.

$$W_R = \left[\left(\frac{\partial R}{\partial x_1} w_1\right)^2 + \left(\frac{\partial R}{\partial x_2} w_2\right)^2 + \left(\frac{\partial R}{\partial x_3} w_3\right)^2 + \cdots \ldots \ldots \ldots + \left(\frac{\partial R}{\partial x_n} n\right)^2\right] \quad (1)$$

3. Thermal modelling

Energy balance (Analysis)

The instantaneous thermal efficiency (η) of the SAC is defined as the fraction of the heat transferred to the working fluid (Q_u) to the total solar radiation incident on the absorber surface (Q_{ab}), [23]:

$$\eta = \frac{Q_u}{Q_{ab}} \quad (2)$$

The amount of heat absorbed by the air is estimated as:

$$Q_u = mc_p(T_{a,out} - T_{a,in}) \quad (3)$$

where, c_p is the specific heat capacity of air, $\dot{m}$ is the air flow rate, $T_{a,in}$ and $T_{a,out}$ are the inlet and outlet temperatures of air, respectively.

The amount of radiation incident on the absorber is calculated as:

$$Q_{ab} = AI \quad (4)$$

where, I is the irradiance, A is the collector aperture area.

By applying the net energy balance to the collector, the thermal energy lost (U_L) from the collector to the surroundings can be evaluated. Mathematically, the net thermal loss is the product of a heat transfer coefficient U_L times the difference between the temperature of the absorber plate (T_{abs}) and the ambient temperature (T_{amb}). By applying this energy balance, the thermal loss coefficient (Q_u) can be evaluated as:

$$Q_u = A[I - U_L(T_{abs} - T_{amb})] \quad (5)$$

The physical property of the fluid is determined relative to the average air temperature. The average air temperature is calculated as:

$$T_{av} = \frac{(T_{a,in} + T_{a,out})}{2} \quad (6)$$

The effective heat transfer (Q_{eff}) is evaluated by subtracting the energy consumption of the DC fans (W_{fan}) from the extracted heat, and evaluated as:

$$Q_{eff} = Q_u - (W_{fan}) \quad (7)$$

Thus, the effective efficiency is evaluated as:

$$\eta_{eff} = \frac{Q_{eff}}{Q_{ab}} \tag{8}$$

4. Results and discussion

A series of tests were conducted to evaluate the performance of the SAC with and without a sand coated absorber under controlled laboratory conditions. The experiments were performed at three different mass flow rates (0.01, 0.015, and 0.02 kg/s/m^2) and three different radiation intensities (400, 600 & 800 W/m^2) over a 2-hr period.

4.1. Temporal variation of temperature

Collector and air temperatures for the sand coated absorber at different positions for mass flow rate (m) and radiation intensity (I) of 0.01 kg/s/m^2 and 400 W/m^2, respectively are shown in Figs. 3(a) and (b). The ambient temperature (T_{amb}) was maintained nearly constant during the test period by using air conditioning units. Fig. 3a also presents the temperature of back side insulation (T_{ins}) and glazing (T_{glaz}), inlet air temperature to the absorber ($T_{a,in}$) and outlet air temperature ($T_{a,out}$). After a rapid initial increase, the temperature tends toward a quasi-steady state. Variation in the average absorber temperature at three different locations (inlet ($T_{abs,in}$), middle ($T_{abs,mid}$), and outlet ($T_{abs,out}$)) are shown in Fig. 3(b). It can be seen that the temperature of the absorber near the inlet is low due to higher rate of heat transfer. Further, the magnitudes of the absorber temperature keep on increasing along the downstream, indicating lower rate of heat transfer since air temperature increases due to higher absorbance of heat near the inlet. For m=0.01 kg/s/m^2 and at I=400 W/m^2 the typical values of T_{ins}, T_{glaz}, T_{abs}, and T_{out}, are 26.6ºC, 47.5ºC, 63.2ºC, and 46.4ºC, respectively.

To have a better idea on the absorptivity/reflectivity of the absorber plate, a test was conducted under natural convection mode, by keeping both the absorber plate (plain, sand coated) under solar simulator (Fig. 3c). In general reflectivity of the sand is high. However, it is assumed that the reflectivity of the sand coated absorber is reduced due to the black paint and the non-uniform surface of the absorber. For a period of 2 hours tests, the variation of temperature indicate that, solar absorber plate with sand coating has always at higher temperature, which varies from 1-3 ºC. This indicates that lower reflectivity and higher absorptivity of sand coated absorber. This is in order with the results of Lati et al. [38].

4.2. Variation of average temperature difference

Variations in the temperature difference for collector with and without sand coated absorber with respect to air mass flow rate for three different radiation levels are shown in Figs. 4a to 4c. In the figures ΔT_{air} represents the temperature difference between air inlet and outlet, ΔT_{glaz} represents the temperature difference between the glazing surface and the ambient, and ΔT_{abs} represents the temperature difference between the absorber surface and ambient. Results indicated that with the increase in air mass flow rate all the values of ΔT decreases. The reduction in the value of ΔT_{air} is due to the lower retention time of the travelling fluid. Further, the heat removal capacity of the working fluid increases with increasing the air mass flow rate thus reduce the values of ΔT_{abs} and ΔT_{glaz}. The slope of the curves indicate that the rate of decrease of $\Delta T_{abs}$is slightly higher than the others; this further reduces the gap between ΔT_{abs} and ΔT_{air}, especially at higher values of *m*, indicating better thermal performance of the solar air collector. A comparison of the trend of ΔT indicates that ΔT_{air} is always higher for the sand coated absorber for all radiation levels, with heat transfer rates as high as 17% greater. Conformity of higher heat transfer for sand coated absorber may also be seen in the trend for ΔT_{abs}. Values of ΔT_{abs} for the sand coated absorber are always lower than that of the plain absorber. The maximum reduction is ΔT_{abs} for the sand coated absorber is as high as 11% compared to the plain absorber.

The higher heat transfer rate for the sand coated absorber was attributed to three factors; (i) sand provides higher effective heat transfer area per unit volume and thus increase the heat transfer capacity; [38] (ii) due to the artificial roughness extended by the presence of the sand particles, this helped to break the development of the thermal boundary layer by allowing better recirculation of flow; and (iii) due to the additional surface area provided by the sand particles, this allowed better heat transfer coupled with the reduction of reflection losses due to non-uniformity of the absorber surface. Increases in radiation power 600 to 800 W/m^2 (Fig. 4(b-c)) increases ΔT by 65-80% for both the SACs.

4.3 Variation of pressure drop

The variation of pressure drop (ΔP) for both plain and sand coated absorbers is presented in Fig. 5. It can be seen that the magnitude of ΔP increases continuously with the increase in air flow rate (*m*). This might be due to higher frictional resistance, which in turn increases the requirement of fan power. Furthermore, it is relevant to mention that, due to inclination of the channel, a difference of potential head between the inlet and outlet plays a crucial role, even though part of this is overcome by the chimney effect. Increasing in the value of *m* by 90%, the ΔP is found to

increase by around 50% for the plain absorber. For the sand coated absorber, the pressure drop is 8-11% higher than the plain absorber.

4.4 Variation of effective heat transfer

Figs. 6 (a-d) highlight the temporal variation of the effective heat transfer (Q_{eff}) calculated using Eq (7) for the collectors with and without sand coating. After 60 min, the system tends to reach its steady state, after which the rate of rise of Q_{eff} is insignificant. Furthermore, it can be seen that Q_{eff} is higher at higher flow rates for each radiation level. For the SAC with the sand coated absorber (Fig. 4(a-b)) with the increases in the flow rates from 0.01 to 0.02 kg/s/m^2, Q_{eff} is enhanced by around 77%. For the SAC with the plain absorber, the enhancement is 57% and 70% at the radiation level of 400 and 800 W/m^2, respectively.

4.5 Variation of overall heat loss coefficient

Temporal variations of overall loss coefficient (U_l) are depicted in Fig. 7(a-d) for the collectors with and without the sand coating. The overall heat loss consists of losses through the back and side insulation, and through the glazing. Top loss (including convection and radiation) through the glazing is much higher than the back losses. This might be the reason for a steady state value of overall loss coefficient after a typical value of time period even though the back losses tend to increase continuously with time (refer the temperature variation of glazing and insulation in Fig. 3).

In general, with an increase in the air flow rate the value of U_l decreases monotonically indicating better thermal performance. This is due to a better heat extraction rate at a higher mass flow rate which in turn reduces the heat loss. At higher heat extraction rates by the working fluid, the system temperature remains lower resulting in a lower rate of heat loss from the top and back. It was found that by increasing the air mass flow rate from 0.01 to 0.02 kg/s/m^2 resulted in a decrease in the heat loss coefficient by about 10-12% at 400-800 W/m^2 for SAC with sand coated absorber and 4-9% for the plain absorber.

4.6 Variation of thermal efficiency and output temperature

The performance of the SAC with respect to thermal efficiency (η) and the corresponding output air temperature ($T_{a,out}$) is shown in Fig. 8(a-c). The thermal efficiency of the SAC increases with the increase in mass flow rate under all conditions. Higher heat extraction rate by the working fluid (due to higher thermal capacity of air) is the reason for the same. Thermal efficiency increases at higher mass flow rates for between 0.01 and 0.015 kg/s/m^2, after that the rate of increase decreases. This may be due to the increases in leakage losses in the SAC and the lower

retention time of the fluid. Overall by increasing the flow rate by 90%, at a radiation level of 400 W/m^2, the thermal efficiency for the SAC with plain and sand coated absorber is found to be enhanced by about 25% and 17%, respectively. Thus, to obtain a similar rate of rise in thermal efficiency, the SAC with a sand coated absorber will require a higher fan power to overcome higher frictional losses.

For all values of *m*, the sand coated absorber provides higher thermal efficiencies than that of the plain absorber and is as high as 17%, at radiation level of 400 W/m^2. This is due to better mixing of the fluid and higher absorption and emission of heat. In this case, the higher rate of required fan power for SAC with a sand coated absorber may be overlooked due to the better thermal efficiency.

In general, due to lower retention time of the working fluid for a higher flow rate, the output air temperature ($T_{a,out}$) decreases even though the value of total extracted heat is increased. Results showed that the efficiency of SAC for the plain and sand coated absorber varies from 17-22% and 20-24%, respectively at 400 W/m^2 and the corresponding output temperature variation is between 30 and 32ºC and 31 and 34 ºC. Increases in the radiation level from 400 to 600 and 400 to 800 W/m^2 resulted in enhancements in thermal efficiency by 36-63% for the plain absorber and 30-68% for the sand coated absorber (Fig. 8(b-c)). The maximum value of thermal efficiency for the plain and sand coated SACs is found to be 34 and 41%, respectively.

4.7 Variation of effective thermal efficiency

Performance of the collector with thermal rise parameter is shown in Fig. 9(a-b) in the conventional Hottel-Whillier-Bliss type format. Results indicated that the effective efficiency (η_{eff}) decreases with the increase in performance parameter (*ΔT/I*), indicating better operation at lower performance parameter value. For a fixed insolation (*I*), the lower value of *ΔT* is obtained at higher air mass flow rates similar to the trend observed for the variation of thermal efficiency with respect to air mass flow rate. On the contrary, for a similar range of *ΔT*, increases in insolation (*I*) will result in lower values of $\Delta T/I$. However, higher levels of insolation is limited with the metrological constraints, thus the former method of increase in effective efficiency may be preferred.

The magnitude of η_{eff} for the sand coated absorber (Fig. 9(a)) increases from 0.19-0.24 with decrease in $\Delta T/I$ from 3.3×10^{-2} to 2.6×10^{-2} at a mass flow rate of 0.01 kg/s/m^2. While the same is increased from 0.31-0.38 with decrease in $\Delta T/I$ from 2.7×10^{-2} to 2.0×10^{-2} at a mass flow rate of 0.02 kg/s/m^2. Thus, a lower $\Delta T/I$ is preferred to obtain better efficiencies and in the

present study the same is obtained by both increasing the magnitudes of I and the air mass flow rate. For a SAC with plain absorber, η_{eff} and $\Delta T/I$ vary between 0.15-0.33 and 1.5-3.2×10^{-2}, respectively (see Fig 7 (b). The sand coated absorber provided better effective thermal efficiency for the same mass flow rate.

A linear correlation between η_{eff} and $\Delta T/I$ is proposed for the SAC with and without absorber using the experimental results. The accuracy of the correlation is determined with the help of a correlation coefficient (CC) and the coefficient of determination (R^2). It is well known that the higher the value of CC and R^2, the correlation is more accurate. Along with the experimental data the correlated data are also plotted in Fig. 9. The CC varies between 0.992 and 0.996, and the R^2 lies within 0.8-0.98. The proposed correlations and the coefficient values are presented in Table 3.

5. Conclusion

The thermal performance of solar air collectors (SAC) with plain and sand coated absorbers was been carried out under controlled laboratory conditions for radiation levels of 400, 600, and 800 W/m^2 and air flow rate ranging between 0.01-0.02 kg/s/m^2. The following observations are made:

- The difference of air temperature between inlet and outlet increases by 66% for increases in radiation levels from 400 to 800 W/m^2 for a sand coated absorber.
- The surface temperature of the sand coated absorber is 4-7% lower than that of plain absorber due to a larger surface area at the same radiation level, indicating higher rate of absorption and emission. Furthermore, the temperature difference of the air between the inlet and outlet for the sand coated absorber is higher by 11% compared to the plain absorber, despite a lower absorber surface temperature.
- The increase in the surface roughness due to the sand coating on the absorber increases the pressure drop by around 8-11% compared to the plain absorber thus requiring higher fan power input.
- The effective heat transfer of the sand coated absorber is always higher than that of the plain absorber and the difference increases with air flow rate. The magnitude of difference ranges between 21-24%.
- Overall the heat loss coefficient for the sand coated absorber is slightly higher than the plain absorber and tends to decrease with increases in the air flow rate and level of radiation.

- The thermal efficiency of the SAC increases with increases in the air flow rate, and the rate of increase for the sand coated absorber is higher than the plain absorber. The maximum increase of 20% and 24% are observed for the plain and sand coated absorber, respectively at 800W/m^2.
- The thermal efficiency of the SAC varies from 17-34% and 20-41% for plain and sand coated absorbers, respectively.
- The sand coating on the absorber improves the thermal efficiency of the SAC. Overall at radiation levels of 800 W/m^2 and mass flow rate of 0.02 kg/s/m^2, the sand coated absorber provides 17.6% higher thermal efficiency compared to the plain absorber.
- The effective efficiency of SACs tends to be enhanced with the decrease in the temperature rise parameter. In general the sand coated absorber provides better effective efficiency than the plain absorber.

References

[1] A. A. Hegazy, "Thermohydraulic performance of air heating solar collectors with variable width, flat absorber plates," *Energy Convers. Manag.*, vol. 41, no. 13, pp. 1361–1378, 2000.

[2] A. L. Hernández and J. E. Quiñonez, "Analytical models of thermal performance of solar air heaters of double-parallel flow and double-pass counter flow," *Renew. Energy*, vol. 55, pp. 380–391, 2013.

[3] R. Vaziri, M. Ilkan, and F. Egelioglu, "Experimental performance of perforated glazed solar air heaters and unglazed transpired solar air heater," *Sol. Energy*, vol. 119, pp. 251–260, 2015.

[4] F. Aissaoui, A. Benmachiche, A. Brima, and D. Belloufi, "Experimental and Theoretical Analysis on Thermal Performance of the Flat Plate Solar Air Collector," *Int. J. Heat Technol.*, vol. 34, no. 2, pp. 213–220, 2016.

[5] I. Soriga and V. Badescu, "Thermal inertia of flat-plate solar collectors in different radiative regimes," *Energy Convers. Manag.*, vol. 111, pp. 27–37, 2016.

[6] C. Sun, Y. Liu, C. Duan, Y. Zheng, H. Chang, and S. Shu, "A mathematical model to investigate on the thermal performance of a flat plate solar air collector and its experimental verification," *Energy Convers. Manag.*, vol. 115, pp. 43–51, 2016.

[7] A. S. Abdullah and Z. M. Omara, "Performance evaluation of plastic solar air heater with different cross sectional configuration," *Appl. Therm. Eng.*, 2017.

[8] H. Caliskan, "Energy, exergy, environmental, enviroeconomic, exergoenvironmental (EXEN) and exergoenviroeconomic (EXENEC) analyses of solar collectors," *Renew.*

Sustain. Energy Rev., vol. 69, no. November 2016, pp. 488–492, 2017.

[9] A. E. Kabeel, M. H. Hamed, Z. M. Omara, and A. W. Kandeal, "Solar air heaters: Design configurations, improvement methods and applications – A detailed review," *Renew. Sustain. Energy Rev.*, 70, no. November 2016, pp. 1189–1206, 2017.

[10] S. Debnath, J. Reddy, Jagadish, and B. Das, "An Expert system based modeling and optimization of SAC for North Eastern India" J Mech. Sci. Tech., 33(8), pp. 1-9, 2019.

[11] A. M. Lanjewar, J. L. Bhagoria, and M. K. Agrawal, "Review of development of artificial roughness in solar air heater and performance evaluation of different orientations for double arc rib roughness," *Renew. Sustain. Energy Rev.*, vol. 43, pp. 1214–1223, 2015.

[12] T. Alam and M. H. Kim, "A critical review on artificial roughness provided in rectangular solar air heater duct," *Renew. Sustain. Energy Rev.*, 69, pp. 387–400, 2017.

[13] B. N. Prasad. and J. S. Saini, "Effect of artificial roughness on heat transfer and friction factor in a solar air heater," *Sol. Energy*, vol. 41, no. 6, pp. 555–560, 1988.

[14] A. A. El-Sebaii, S. Aboul-Enein, M. R. I. Ramadan, S. M. Shalaby, and B. M. Moharram, "Investigation of thermal performance of-double pass-flat and v-corrugated plate solar air heaters," *Energy*, vol. 36, no. 2, pp. 1076–1086, 2011.

[15] C. D. Ho, H. M. Yeh, and T. C. Chen, "Collector efficiency of upward-type double-pass solar air heaters with fins attached," *Int. Commun. Heat Mass Transf.*, vol. 38, no. 1, pp. 49–56, 2011.

[16] C. D. Ho, H. Chang, R. C. Wang, and C. S. Lin, "Performance improvement of a double-pass solar air heater with fins and baffles under recycling operation," *Appl. Energy*, vol. 100, pp. 155–163, 2012.

[17] H. Benli, "Experimentally derived efficiency and exergy analysis of a new solar air heater having different surface shapes," *Renew. Energy*, vol. 50, pp. 58–67, 2013.

[18] R. K. Ravi and R. P. Saini, "Nusselt number and friction factor correlations for forced convective type counter flow solar air heater having discrete multi V shaped and staggered rib roughness on both sides of the absorber plate," *Appl. Therm. Eng.*, 2017.

[19] A. E. Kabeel, A. Khalil, S. M. Shalaby, and M. E. Zayed, "Experimental investigation of thermal performance of flat and v-corrugated plate solar air heaters with and without PCM as thermal energy storage," *Energy Convers. Manag.*, vol. 113, pp. 264–272, 2016.

[20] C. D. Ho, C. F. Hsiao, H. Chang, and Y. E. Tien, "Investigation of Device Performance for Recycling Double-pass V-corrugated Solar Air Collectors," *Energy Procedia*, vol. 105, pp. 28–34, 2017.

[21] A. E. Kabeel, M. H. Hamed, Z. M. Omara, and A. W. Kandel, "On the performance of a

baffled glazed-bladed entrance solar air heater," *Appl. Therm. Eng.*, 2018.

[22] S. Şevik and M. Abuşka, "Thermal performance of flexible air duct using a new absorber construction in a solar air collector," *Appl. Therm. Eng.*, 2018.

[23] S. Debnath, B. Das, P. R. Randive, and K. M. Pandey, *Performance of solar air collector in the climatic condition of North Eastern India*. Energy, 165, 281-298, 2018.

[24] A. Boulemtafes-Boukadoum and A. Benzaoui, "CFD based analysis of heat transfer enhancement in solar air heater provided with transverse rectangular ribs," *Energy Procedia*, vol. 50, pp. 761–772, 2014.

[25] R. Kumar, V. Goel, and A. Kumar, "Investigation of heat transfer augmentation and friction factor in triangular duct solar air heater due to forward facing chamfered rectangular ribs: A CFD based analysis," *Renew. Energy*, vol. 115, pp. 824–835, 2018.

[26] S. K. Sharma and V. R. Kalamkar, "Experimental and numerical investigation of forced convective heat transfer in solar air heater with thin ribs," *Sol. Energy*, vol. 147, pp. 277–291, 2017.

[27] H. Yeh and C. Ho, "Solar air heaters with external recycle," *Appl. Therm. Eng.*, vol. 29, no. 8–9, pp. 1694–1701, 2009.

[28] H. Yeh and C. Ho, "Downward-type solar air heaters with internal recycle," *J. Taiwan Inst. Chem. Eng.*, vol. 42, no. 2, pp. 286–291, 2011.

[29] P. Naphon, "On the performance and entropy generation of the double-pass solar air heater with longitudinal fins," *Renew. Energy*, vol. 30, pp. 1345–1357, 2005.

[30] A. A. Mohamad, "High efficiency solar air heater," *Sol. Energy*, vol. 60, no. 2, pp. 71–76, 1997.

[31] F. Ozgen, M. Esen, and H. Esen, "Experimental investigation of thermal performance of a double-flow solar air heater having aluminium cans," *Renew. Energy*, vol. 34, no. 11, pp. 2391–2398, 2009.

[32] A. P. Omojaro and L. B. Y. Aldabbagh, "Experimental performance of single and double pass solar air heater with fins and steel wire mesh as absorber," *Appl. Energy*, vol. 87, no. 12, pp. 3759–3765, 2010.

[33] M. Abuşka and M. B. Akgül, "Experimental Study on Thermal Performance of a Novel Solar Air Collector Having Conical Springs on Absorber Plate," *Arab. J. Sci. Eng.*, vol. 41, no. 11, pp. 4509–4516, 2016.

[34] M. Abuşka, "Energy and exergy analysis of solar air heater having new design absorber plate with conical surface," *Appl. Therm. Eng.*, 2017.

[35] M. Ansari and M. Bazargan, "Optimization of Flat Plate Solar Air Heaters with Ribbed

Surfaces," *Appl. Therm. Eng.*, no. February, 2018.

[36] P. Velmurugan and R. Kalaivanan, "Energy and exergy analysis of solar air heaters with varied geometries," *Arab. J. Sci. Eng.*, vol. 40, no. 4, pp. 1173–1186, 2015.

[37] A. Ahmadi, D. D. Ganji, and F. Jafarkazemi, "Analysis of utilizing Graphene nanoplatelets to enhance thermal performance of flat plate solar collectors," *Energy Convers. Manag.*, vol. 126, pp. 1–11, 2016.

[38] M. Lati, S. Boughali, D. Bechki, H. Bouguettaia, D. Mennouche, N. Gana & S. Ghettas, "Experimental investigation on effect of an absorber plate covered by a layer of sand on the efficiency of passive solar air collector", *Int. J Green Energy*, DOI: 10.1080/15435075.2019.1577740

Table 1. List of earlier works on solar air collector.

Authors	Mass flow rate	Flow pass	Glazing no. and material	Dimensions of the collector	Air gap	Absorber	Remarks	Thermal efficiency
Hernández and Quiñonez [2]	0.01-0.1 kg/s	Single and double pass, Double flow: parallel and counter	02, Polycarbonate	2 m×0.9 m	0.025 m	Flat plate	• For double flow SAC, with same inlet condition, mass flow rate of air in the channel between the absorber and the glazing is higher than at the bottom channel between the absorber and insulation. • At higher mass flow rate double parallel flow is better than double counter flow collector.	0.49-0.62
Vaziri et al. [3]	0.017-0.036 kg/s	Single pass flow	01, Plexi glass perforated with 0.003 m hole	0.9m×0.9 m	0.03m	Flat plate with black, green, blue, red, violet, light yellow and white colour	• Thermal efficiency of perforated glazed solar air heaters (PGSAH) increases with mass flow rate. • Black colour absorber provided highest efficiency than other 6 colour. • PGSAH provided better performance than unglazed one.	0.55-0.85
Aissaoui et al. [4]	0.1324 kg/s	Single pass between the absorber and bottom plate	01, glass	2m×1m	-	Flat plate black coated	• Thermal efficiency increased with the solar intensity (400-900W/m^2) • Computational and experimental convection coefficient compared	0.22-0.4
Sun et al. [6]	0.02-0.03 kg/s	Single pass	-	2m×2m	0.08m	Flat plate black coated	• During experimentation with radiation of 800W/m^2 thermal efficiency varied from 0.56 to 0.64, increases with increase in mass flow rate. • Computational study is performed for mass flow rate of 0.02-0.05 kg/s. Maximum efficiency of 0.54 was obtained at 0.04 kg/s at radiation of 700 W/m^2. • Beyond mass flow rate of 0.04kg/s, efficiency did not increase significantly. Also tend to reduce at lower intensity of radiation.	Experiment: 0.56-0.64 Computational: 0.35-0.55
Abdullah et al. [7]	0.05-0.25 kg/s	Single pass	Single (flat, triangular, semi	5m ×1.25m	-	Semi-circular having ϕ1.25m	• The highest efficiencies of 80% were achieved for the circular configuration	0.45-0.85

			circular)				(semi-circular absorber and semi-circular transparent cover) with a flow rate of 0.18 kg/s and average solar radiation of 925 W/m^2.	
Debnath et al. [10]	0.0039 to 0.0118 kg/s	Single pass	01-02, glass	1.52 m x 0.52 m x	0.045-0.055 m	Flat plate & wavy plate	• Double glazing provided better thermal performance • Optimum performance was predicted through expert system at mass flow of 0.00785 kg/s, inclination 45°, radiation level of 583 W/m^2. • Wavy absorber provided better thermal performance than flat plate SAC.	26-38%
Benli et al. [17]	0.02-0.05 kg/s	Single pass	Single glass	0.70 m × 0.7 m	-	Flat, corrugate, reverse corrugate, trapeze, and reverse trapeze	• Efficiency of the collector varied from 5-55% for corrugate, from 22-46% for reverse corrugate, from 20-42% for trapeze, from 15-28% for reverse trapeze and between 7% and 17% for flat plate absorber under similar working condition • Increase in mass flow rate from 0.02-0.5 kg/s, friction coefficient increased by 2.8-fold, 6-fold, 7.6-fold, 9.6-fold and 11.6-fold, for flat-plate, trapeze, reverse trapeze, corrugate, and reverse corrugate, collector.	5-55%
Ravi and Saini [18]	Re=2000 - 20000	Double pass	Single glass	1m ×0.3m	0.025 m	V-shaped, Stagger, Ribbed	• Nusselt number was found to enhance by 4.52 times compared to that of smooth duct. • Friction factor (f) enhanced by 3.13 folds • Correlation proposed to predict the both	-
Kabeel et al. [19]	0.009-0.062 kg/s	Single pass	Single glass	1.0 m x??	0.005 m	Flat and V-corrugated	• Efficiency of the conventional collector was 47% and 40.7%, with and without PCM at a mass flow of 0.062 kg/s. • With PCM, the highest efficiency of the v-corrugated solar heater was 62%, at flow rates 0.062 kg/s.	Flat plate with PCM: 18-47% V-corrugated with PCM: 27-62%
Kabeel et al. [21]	0.013 - 0.04 kg/s	Single pass	Single glass	2m × 1m	0.01 m	Flat, Baffle, Fin	• Thermal efficiency of flat, baffled and finned SAC found to be 57.07, 43.1 and 32.12%, respectively. • Baffles fixed with fin provided highest efficiency of 83.8%.	0.15-0.83

Sevik and Abuska [22]	0.013-0.044 kg/s	Single pass	No glass, single glass	2m × 1m	0.013-0.1 m	Flat, Flexible duct	• The highest thermal efficiency of 81.3% was obtained with flexible duct. • Collector with flexible duct provided 15.9–41.2% higher thermal efficiency. • Increase mass flow rate from 0.013 to 0.04 raised the Nusselt number by 1.7 times.	0.23-0.83
Yeh and Ho [27]	0.01 - 0.02 kg/s	Single pass (internal recycleflow)	Single	0.6 m × 0.6 m	0.05 m	Fin	• Compare to external recycle, internal recycle enhance the thermal performance at higher rate. • Recycle up to 7 nos. increase the efficiency up to 118%.	0.35-0.62
Yeh and Ho [28]	0.01 - 0.02 kg/s	Single pass (external recycle)	Single	0.6 m× 0.6 m	0.05 m	Fin	• Recycle up to 5 nos. increase the efficiency up to 83% compare to traditional no recycle SAC.	0.24-0.45
Naphon [29]	0.02-0.1 kg/s	Double (counter) pass flow	Single glass	2.4 m × 1.2 m	0.15 m	Fin	• Increase in mass flow rate from 0.02 to 0.1 kg/s enhances the thermal efficiency up to 100%. • Increase in fin height from 0.05 to 0.08 m increases the efficiency up to 50%.	0.3-0.58
Ozgen et al. [31]	0.03 - 0.05 kg/s	Double pass flow	Single	2.14 m × 0.84 m			• Canned absorber provided efficiency of up to 72% as for the flat plate SAC up to 51%.	0.21-0.72
Omojaro and Aldabbagh [32]	0.012 - 0.038 kg/s	Single pass, double pass	Single glass	1.0 m ×1.5 m	0.03-0.07 m	Fin	• The highest efficiency of single and double pass collector were 59.62% and 63.74%, respectively, at mass flow rate of 0.038 kg/s.	0.18-0.63
Ansari and Bazargan [35]	Re=1.9-39×10^3	Single pass	Single glass	1.6m × 0.073 m	0.073 m	Flat and ribbed	• At lower flow rate (Re=0.5×10^4) ribs improve the efficiency up to 20%. • At around Re=2.0×10^4 optimum thermal efficiency was observed • At higher flow rate (Re=2.0×10^4) the performance of the flat absorber was better than ribbed.	Flat: 0.42-0.54 Ribbed: 0.2-0.58
Velmurugan and Kalaivanan [36]	0.01- 0.04 kg/s	Single pass, dual pass	Double glass	2m × 0.46m	-	Flat, Fin, Wire mesh	• Experimental results indicated that that wire meshed double pass SAC provided 13.71–22.86% higher efficiency than traditional SAC.	0.32-0.76

Table 2a: Accuracy and percentage errors for various instruments

Instrument	Accuracy	Range	% error
T-type thermocouple	± 0.5^{0}C	0 – 300 ^{0}C	1.25
Pyranometer	± 5 W/m^2	0 – 4000 W/m^2	2.5
Anemometer	± 0.01 m/s	0 – 25 m/s	0.5
Differential manometer	± 0.05 hpa	0-100 hpa	5

Table 2b: Uncertainties of different measurement

Parameter	**% Uncertainties**
Temperature	±0.5
Solar Radiation	±2.5
Velocity	± 0.5
Pressure drop	±5
Efficiency	±2.6

Table 3. Correlation coefficient (CC) and coefficient of determination (R^2) for correlation of effective efficiency.

Flow rate	**CC**	**R^2**
Sand coated absorber		
m=0.01 kg/s/m^2	0.987	0.8916
m=0.015 kg/s/m^2	0.984	0.8455
m=0.02 kg/s/m^2	0.982	0.8093
Plain absorber		
m=0.01 kg/s/m^2	0.995	0.9665
m=0.015 kg/s/m^2	0.994	0.8653
m=0.02 kg/s/m^2	0.996	0.9874

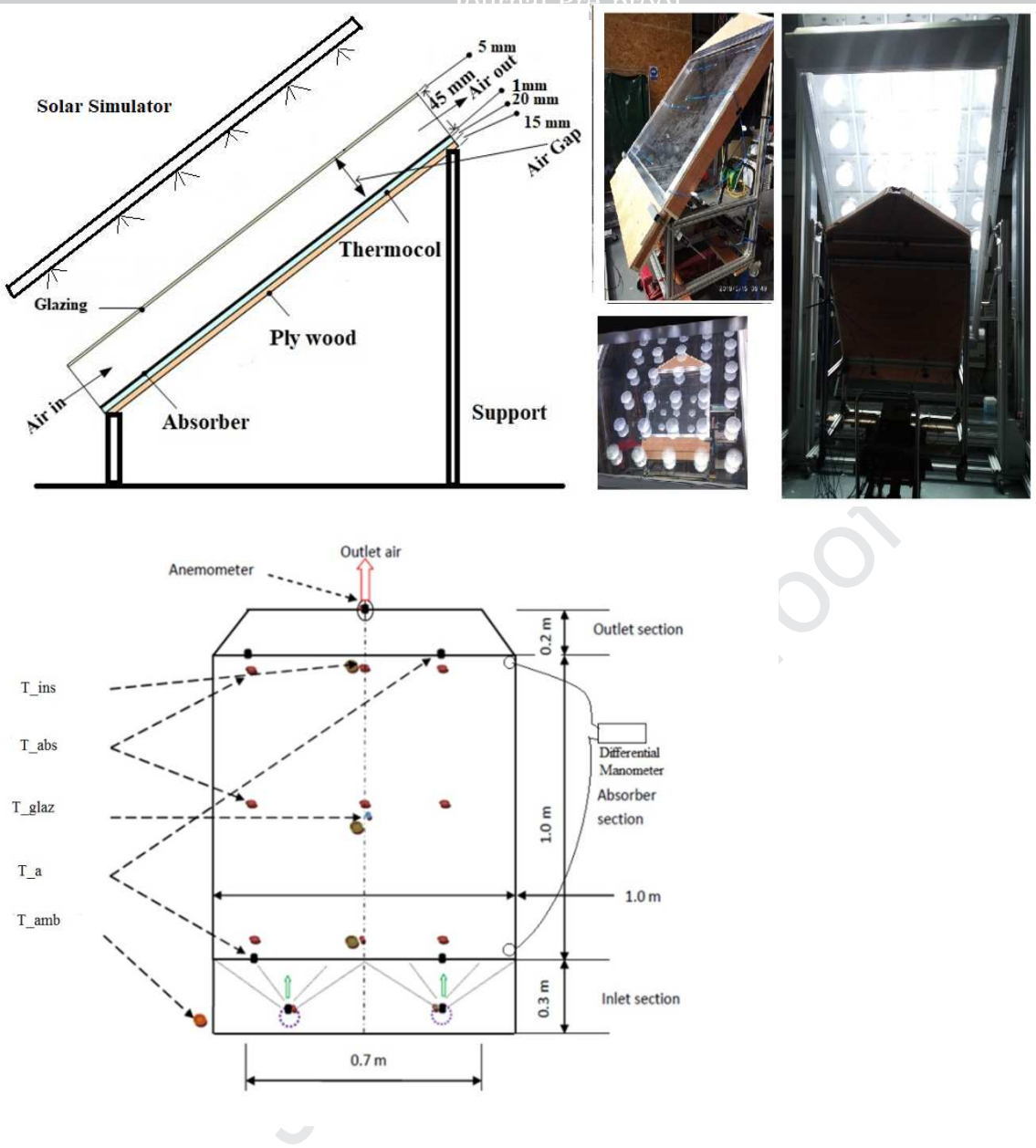

Fig. 1. Detail of the tested solar air collector, including temperature sensor positions.

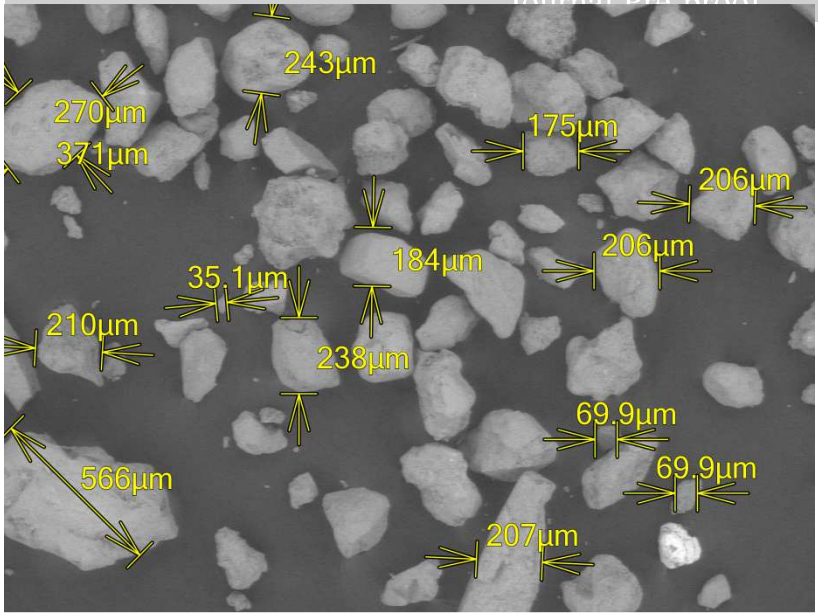

Fig. 2 SEM image of used sand.

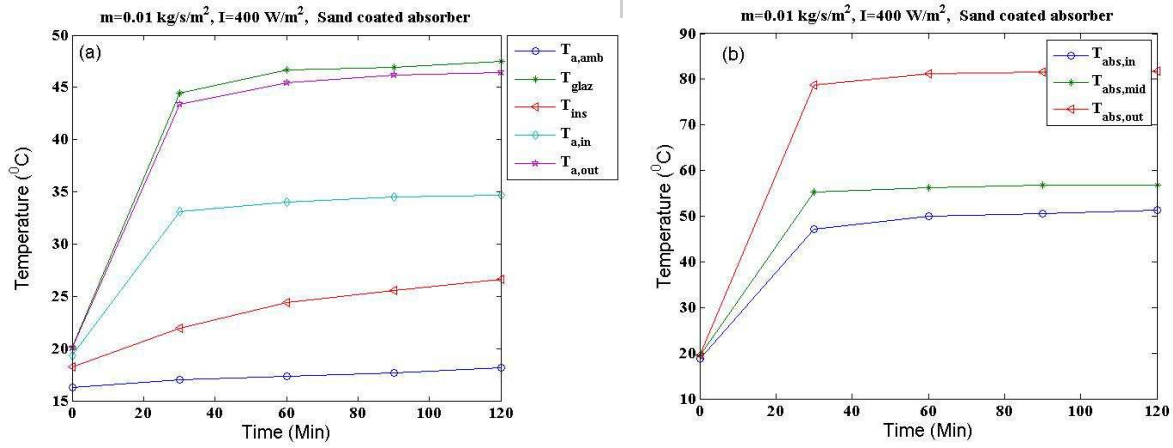

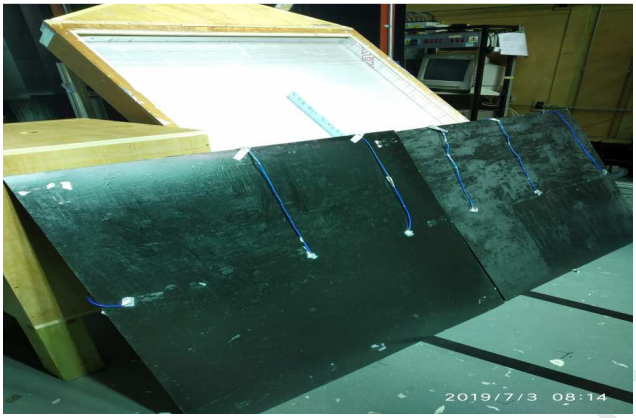

(c)

Fig. 3. Variation in temperatures at different positions within the collector at air mass flow rate of 0.01 kg/s/m^2 for the sand coated absorber: (a) air, glazing, and insulation temperature; (b) absorber surface temperature at the inlet, middle and outlet; (c) both plain and sand coated absorber plates under the solar simulator under natural convection mode.

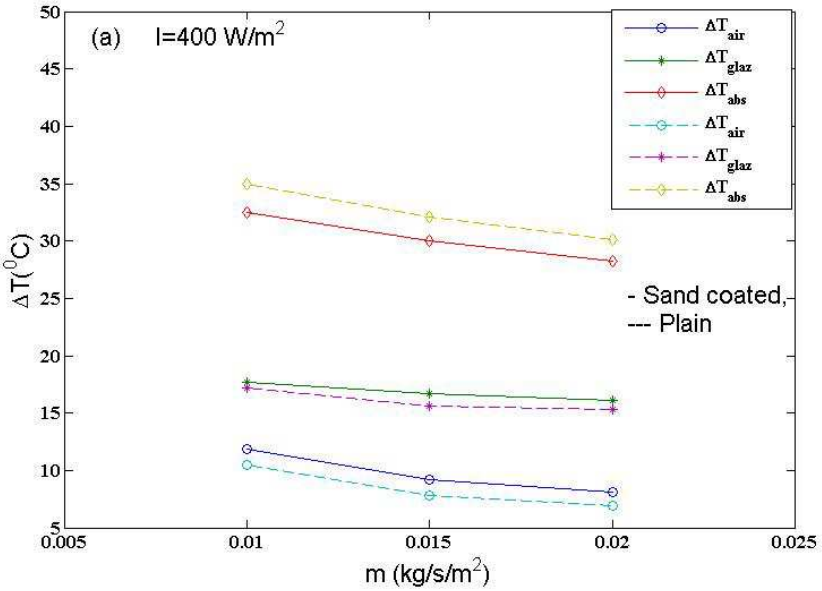
(a) I=400 W/m2
ΔTair
ΔTglaz
ΔTabs
ΔTair
ΔTglaz
ΔTabs
- Sand coated,
--- Plain
ΔT(0C)
m (kg/s/m2)
50
45
40
35
30
25
20
15
10
5
0.005
0.01
0.015
0.02
0.025

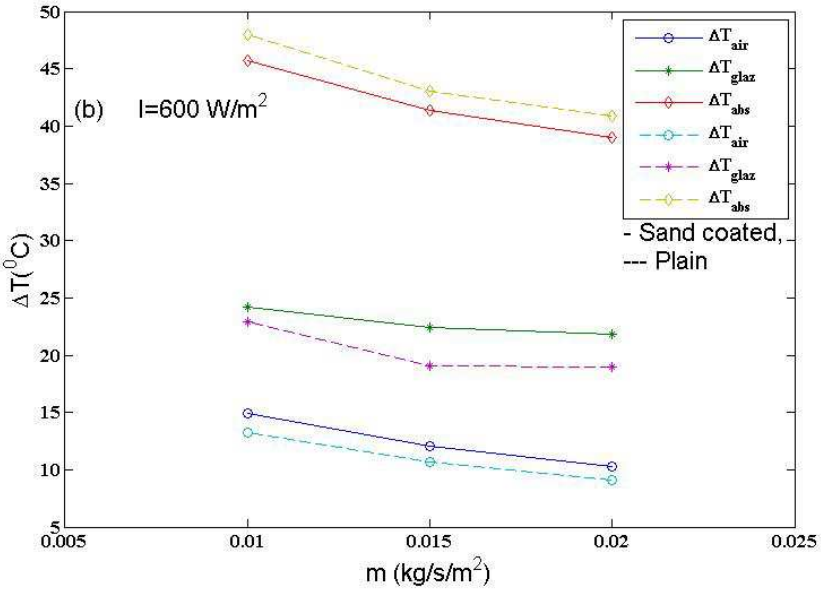
(b) I=600 W/m2
ΔTair
ΔTglaz
ΔTabs
ΔTair
ΔTglaz
ΔTabs
- Sand coated,
--- Plain
ΔT(0C)
m (kg/s/m2)
50
45
40
35
30
25
20
15
10
5
0.005
0.01
0.015
0.02
0.025

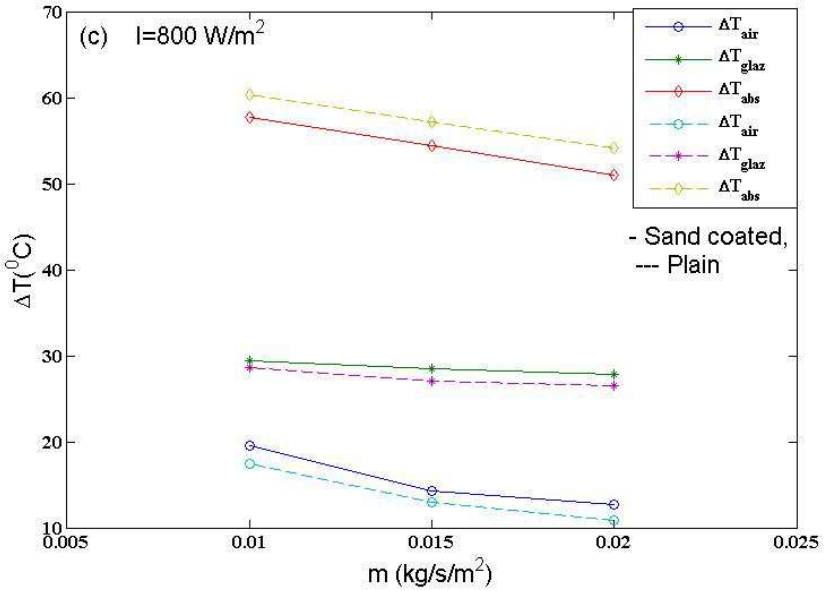

Fig. 4. Variation in temperature difference (ΔT) for the collector with plain (dotted line) and sand coated (continuous line) absorbers with respect to air mass flow rate (m) at (a) 400 W/m^2; (b) 600 W/m^2 and (c) 800 W/m^2

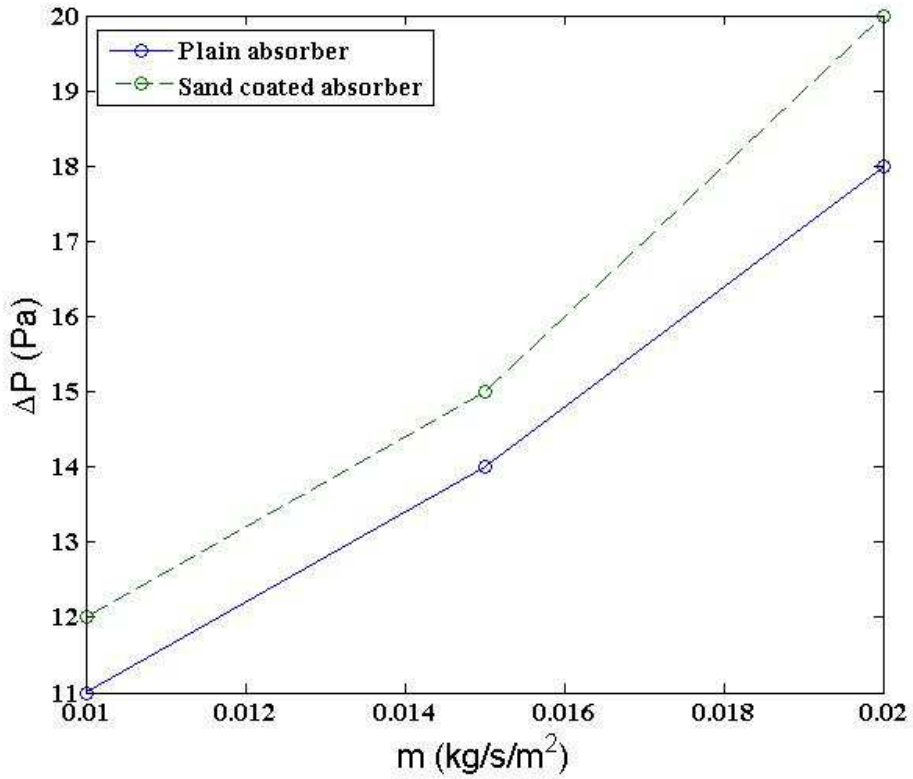

Fig. 5. Variation in pressure drop (*ΔP*) with respect to air mass flow rate (*m*) for the absorber with and without sand coating.

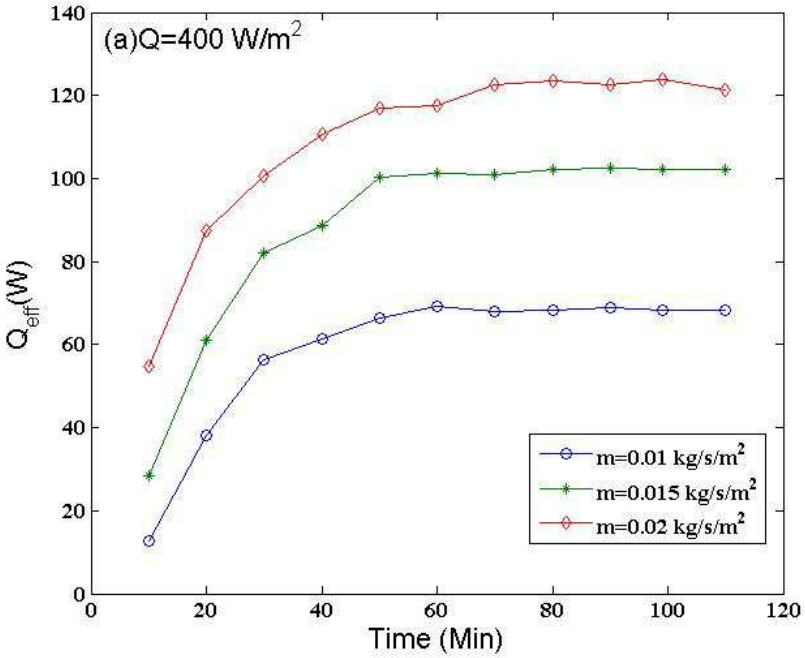
(a)Q=400 W/m2
Qeff(W)
Time (Min)
m=0.01 kg/s/m2
m=0.015 kg/s/m2
m=0.02 kg/s/m2

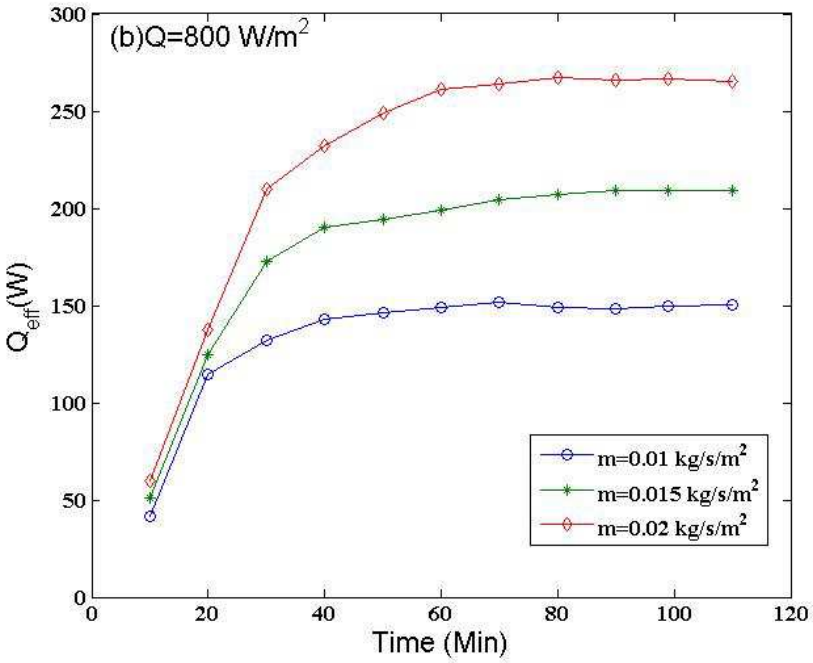
(b)Q=800 W/m2
Qeff(W)
Time (Min)
m=0.01 kg/s/m2
m=0.015 kg/s/m2
m=0.02 kg/s/m2

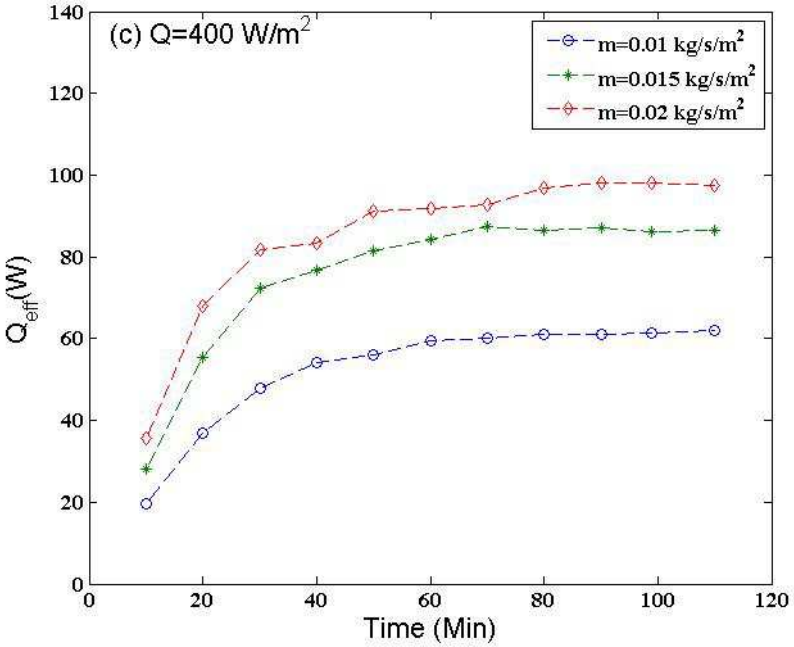

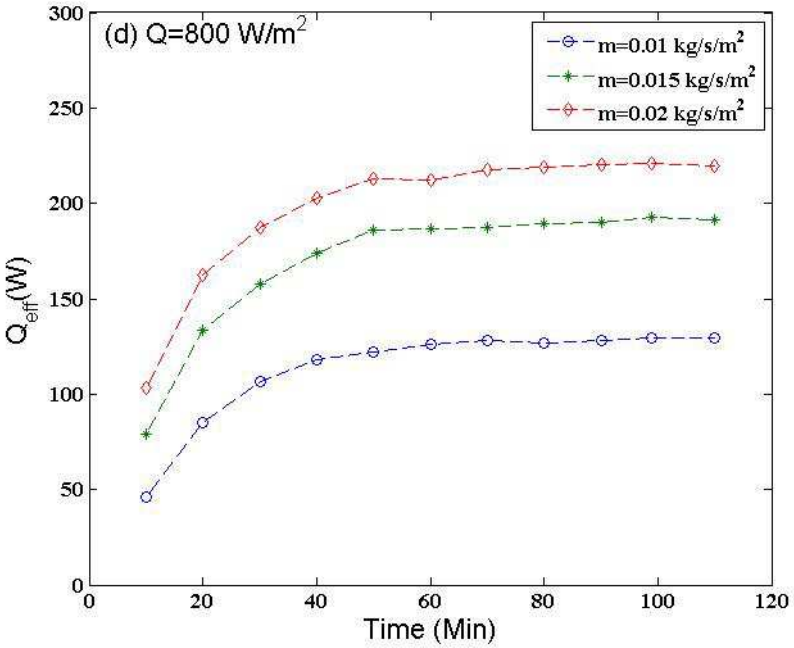

Fig. 6. Variation of effective heat transfer (Q_{eff}) within the test period for different air mass flow rates (m): (a) Sand coated at 400 W/m^2 (b) Sand coated at 800 W/m^2 (c) Plain absorber at 400 W/m^2 (d) Plain absorber at 800 W/m^2.

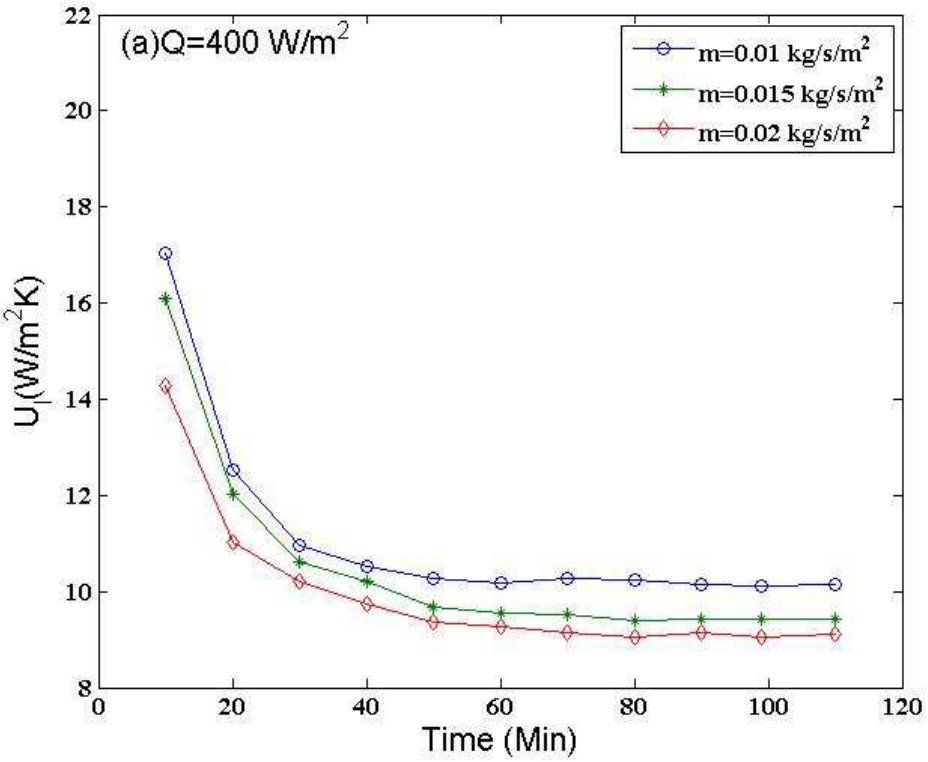
(a)Q=400 W/m2
m=0.01 kg/s/m2
m=0.015 kg/s/m2
m=0.02 kg/s/m2
U(W/m2K)
Time (Min)
22
20
18
16
14
12
10
8
0
20
40
60
80
100
120

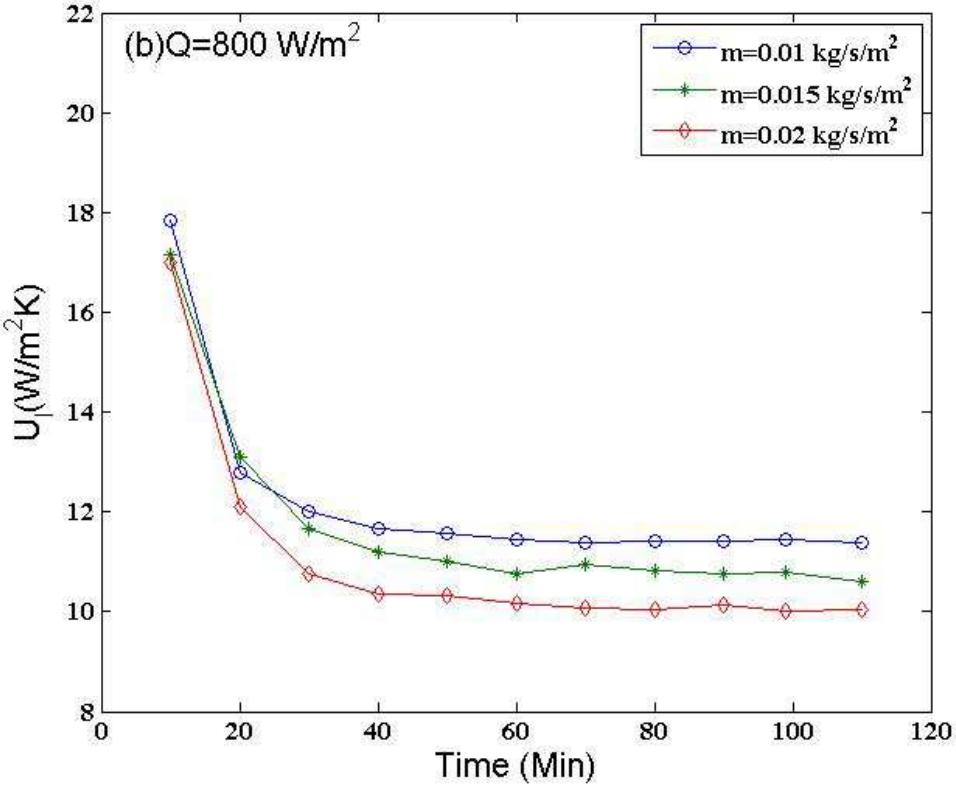
(b)Q=800 W/m2
m=0.01 kg/s/m2
m=0.015 kg/s/m2
m=0.02 kg/s/m2
U(W/m2K)
Time (Min)
22
20
18
16
14
12
10
8
0
20
40
60
80
100
120

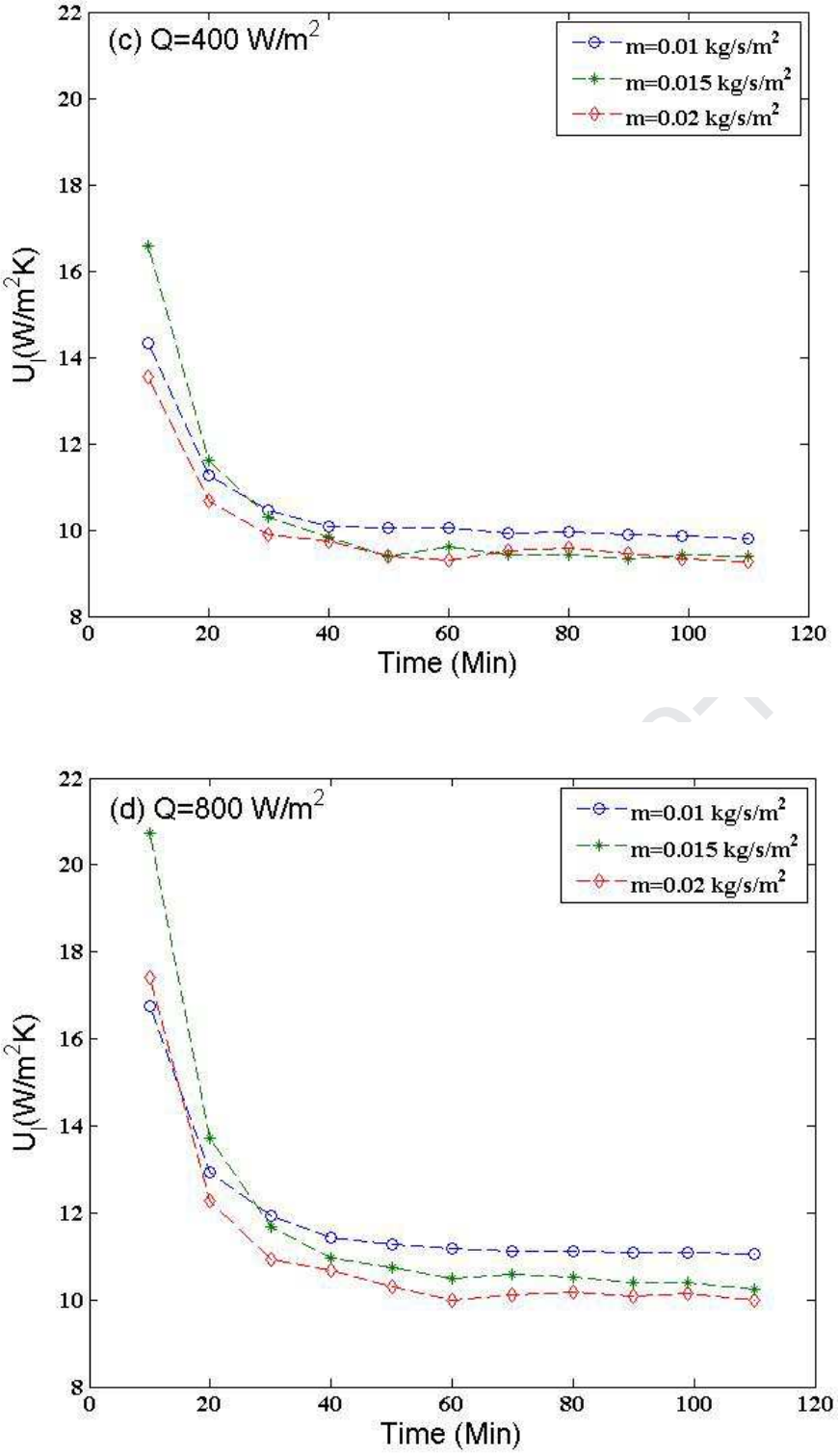

Fig. 7. Variation in overall heat loss coefficient (U_l) within the test period for different air mass flow rates (m). (a) Sand coated at 400 W/m^2 (b) Sand coated at 800 W/m^2 (c) Plain absorber at 400 W/m^2 (d) Plain absorber at 800 W/m^2.

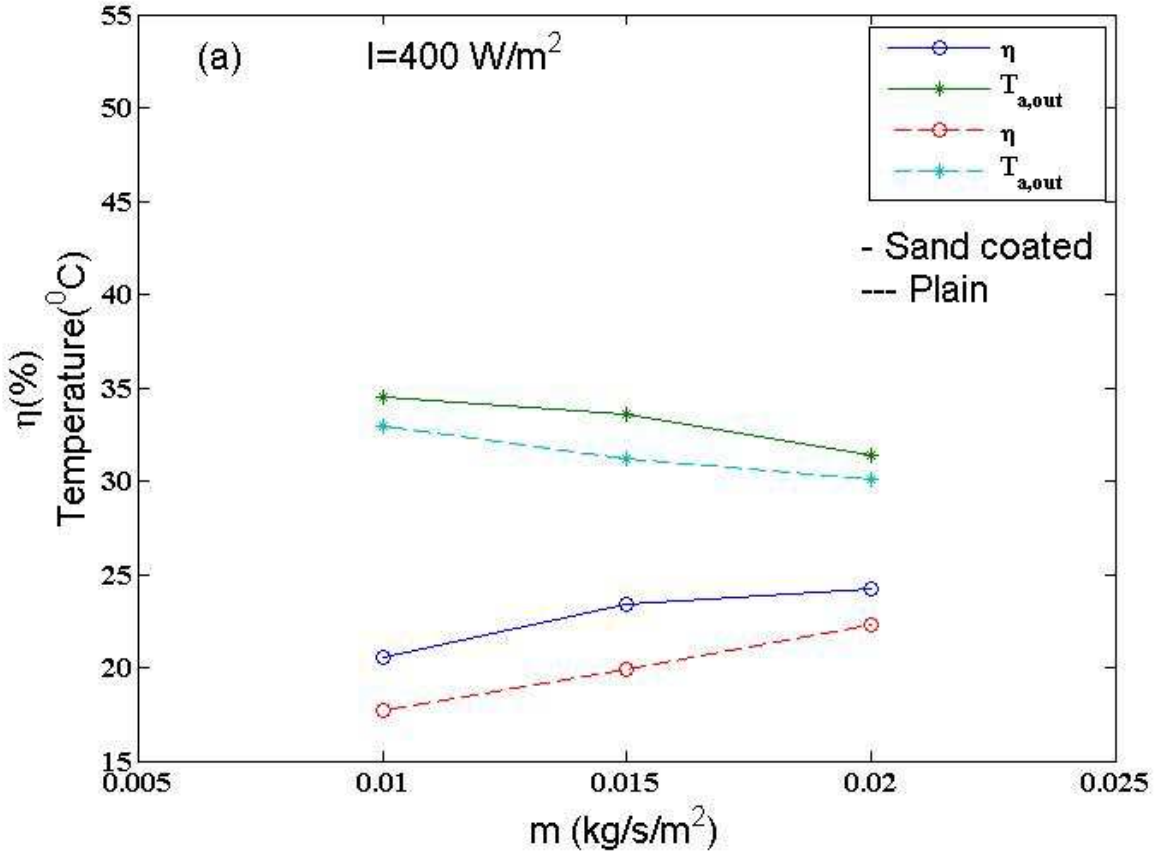
(a)
I=400 W/m2
η
Ta,out
η
Ta,out
- Sand coated
--- Plain
η(%)
Temperature(0C)
m (kg/s/m2)
55
50
45
40
35
30
25
20
15
0.005
0.01
0.015
0.02
0.025

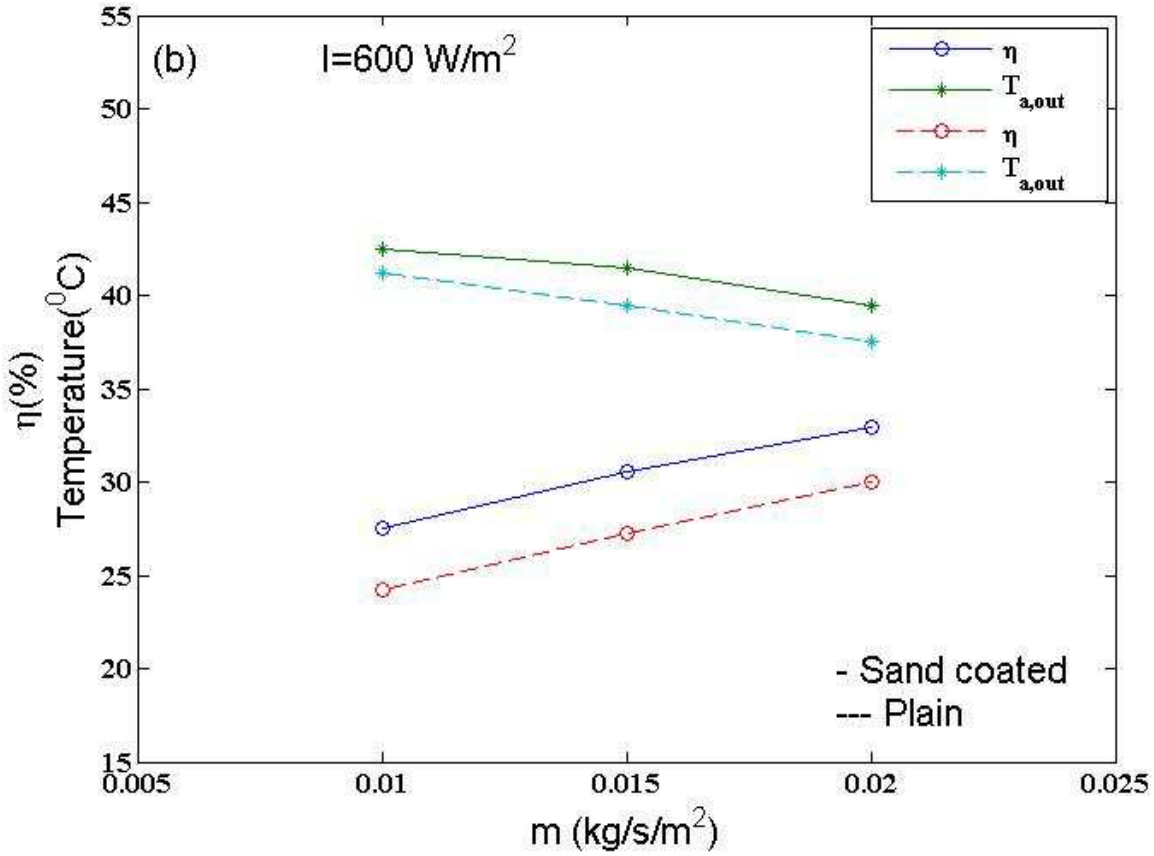
(b)
I=600 W/m2
η
Ta,out
η
Ta,out
- Sand coated
--- Plain
η(%)
Temperature(0C)
m (kg/s/m2)
55
50
45
40
35
30
25
20
15
0.005
0.01
0.015
0.02
0.025

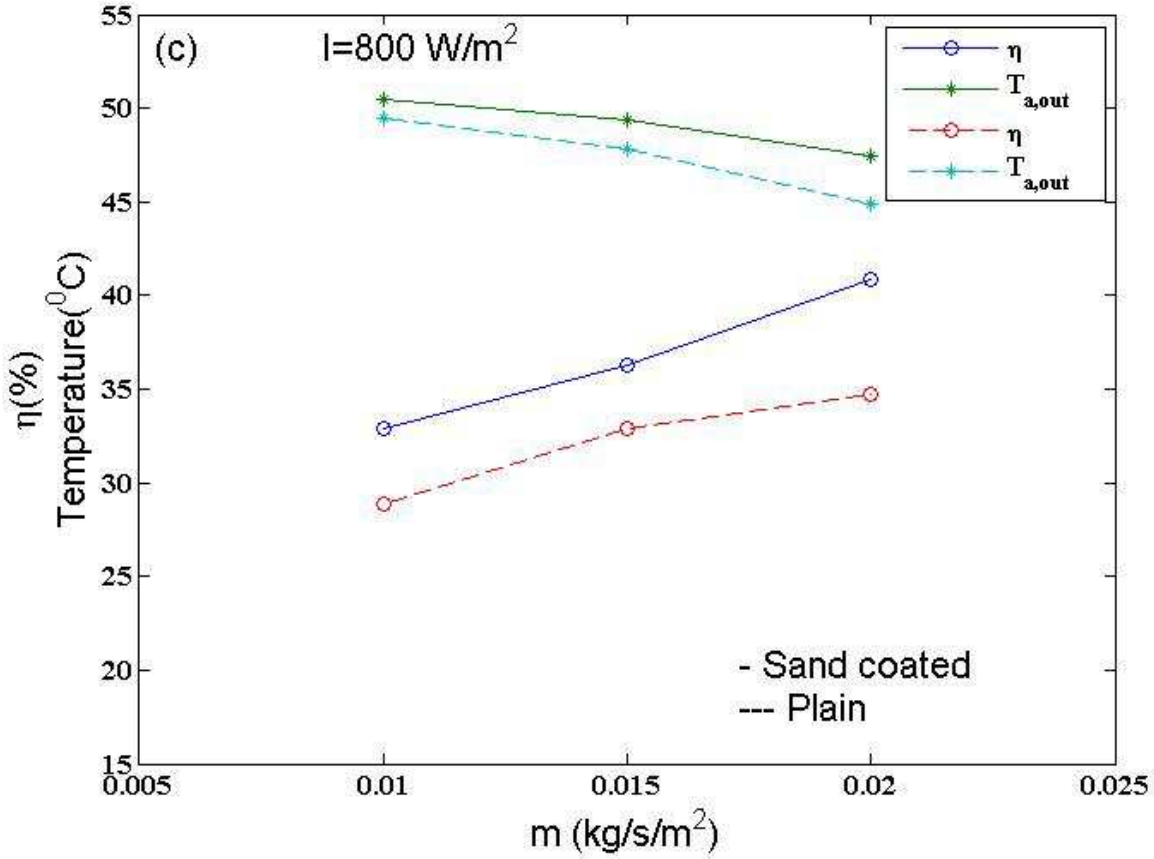

Fig. 8. Variation in thermal efficiency and outlet temperature of the SAC with plain and sand coated absorbers with respect to air mass flow rate at (a) 400 W/m^2 (b) 600 W/m^2 (c) 800 W/m^2.

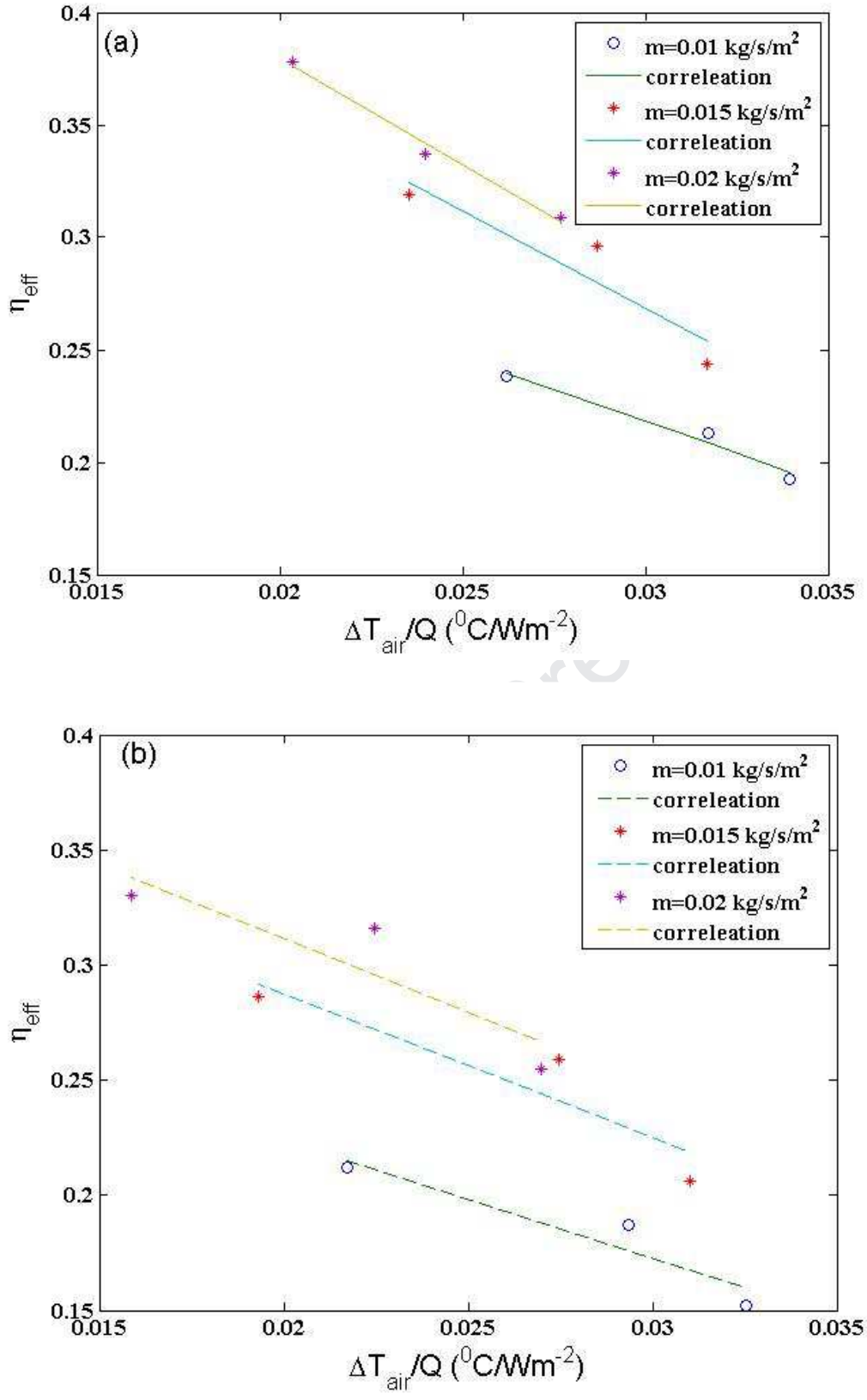

Fig. 9. Experimental and correlated data for the effective thermal efficiency with respect to temperature rise parameters for SAC. (a) sand coated absorber; (b) plain absorber.

Highlights:

- Performance of solar air collector (SAC) with sand coated absorber is presented
- Increase in air flow rate by 90% enhance efficiency by 68% for plain absorber
- SAC with sand coated absorber provides 17% higher efficiency than plain absorber
- The absolute thermal efficiency of the SAC varied from 19% to 41%
- Low cost addition of a layer of sand coating improves thermal performance of SAC

Declaration of interests

√☐ The authors declare that they have no known competing financial interests or personal relationships that could have appeared to influence the work reported in this paper.

☐The authors declare the following financial interests/personal relationships which may be considered as potential competing interests: